Catabot: Autonomous Surface Vehicle with an Optimized Design for Environmental Monitoring

Mingi Jeong, Monika Roznere, Samuel Lensgraf, Amy Sniffen,
Devin Balkcom, Alberto Quattrini Li
Department of Computer Science, Dartmouth College, Hanover, NH, USA
mingi.jeong.gr@dartmouth.edu, monika.roznere.gr@dartmouth.edu, samuel.e.lensgraf.gr@dartmouth.edu,
amy.k.sniffen.gr@dartmouth.edu, devin.balkcom@dartmouth.edu, alberto.quattrini.li@dartmouth.edu

***Abstract*—This paper presents an optimized design of research-oriented ASVs and a systematic design evaluation methodology for reliable in-water sensing. The objective is to minimize the interference on sensor readings by any ASV maneuver. The design space includes motors and sensors locations. In addition, this paper analyzes modularity – i.e., the effects of new sensor's installation. All prototype designs are thoroughly tested using hydrostatic analyses, Computational Fluid Dynamics (CFD) simulations, and real-world field testings. Quantitative metrics, including trim, pitch, velocity magnitude of flow, and turbulence, are used to compare different configurations. Our experiments show that a motor configuration at the back part of the straights hulls is the most optimal design, resulting in high-quality data collection.**

***Keywords*—Autonomous Surface Vehicle, Computational Fluid Dynamics, Design Optimization, Environmental Monitoring, In-water Sensor Interference**

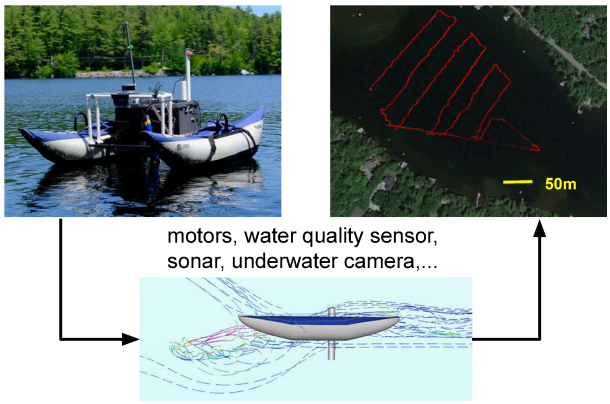

Fig. 1: The design of a research-oriented ASV for monitoring tasks is optimized by finding the locations of motors and in-water sensors that minimize interference on data measurements.

I. Introduction

This paper proposes a novel fit-for-purpose design and systematic evaluation methodology for a research-oriented Autonomous Surface Vehicle (ASV) to reliably collect measurements in aquatic environments. The ASV design is optimized for motion efficiency and for in-water high-quality sensing (see Fig. 1).

Recent developments and applications of ASVs show promising results in reducing time and efforts for tasks normally handled by human beings. Important examples include: environmental monitoring, search and rescue, and military operations. In response to climate and environmental changes, scientists are increasingly deploying ASVs to collect data and monitor our marine ecosystems. However, more evaluation on the ASV design is required to ensure monitoring tasks are performed with reliable data collection. When the data quality is low, sensor or electronic configurations need to be altered, resulting in additional manual labor: re-design, redeployment, and additional verification.

The reason for this low data quality problem is that ASVs are built following typical ship design criteria and rules [1]–[3], focusing on maneuvering performance or safety, unrelated to the main mission of the ASVs. Therefore, current approaches to the development of research-oriented ASVs [4]–[8] do not include a quantitative analysis between their design and sensing performance. This lack of analysis raises questions on whether the motion stability, the sensor data quality, and the task efficiency can be improved, e.g., in coral reef surveying or in water quality monitoring.

This paper provides the following main contributions:

- A modular research-oriented ASV design.
- An optimization procedure for a particular design space – locations of motors and sensors – that is based on the proposed ASV design.
- A new systematic validation scheme and metrics that provide qualitative and quantitative analyses on sensor interference.
- Experiments conducted in simulation and in real-world environments.

The proposed novel analysis ensures that the designed ASV will effectively complete its task and collect high-quality in-water data, which can then be used for scientific research. The validation is performed through Computational Fluid Dynamics (CFD) simulations and field tests for operational reliability in sea waters (location of motors) and in lake waters (location of in-water sensors). While insights from this paper can apply for different scenarios, we test sensors for two important tasks: monitoring cyanobacterial blooms in lake waters and coral reef surveying in oceanic environments.

This paper is structured as follows. Section II discusses related works for developing ASVs for the sake of environmental monitoring. Section III addresses essential design

 DOI: 10.1109/IEEECONF38699.2020.9389391

components and detailed descriptions of on-board parts of our ASV: hull, propulsion, computer and communication system, sensors and design space. Section IV presents our analysis on sensor interference on both simulations and field tests in sea waters and in lake waters, depending on different designs and configurations. Section V discusses the final decision on the research-oriented design from qualitative and quantitative results. Finally, experimental insights and future works are discussed in Section VI.

II. Related Work

Design and build of ASVs have been studied [4], [5], [7]–[19] for decades since the first prototype ASV ARTEMIS [20]. In literature, the main dimensions for the designs of ASVs are seaworthiness, maneuverability, autonomous system components and control. Regarding seaworthiness, technical designs of catamaran-type and monohull-type ASVs were studied by focusing on the hydrostatic validations of their models [9], [10]. Maneuvering characteristics were mainly investigated from station-keeping, stopping distance, zig-zag, and turning radius in compliance with guidance on conventional ships [4], [11], [12]. Autonomous system components and control were primarily discussed by [5], [7], [8], [13]–[19]. Such designs follow the conventional ship standards uncorrelated with their specific tasks.

Currently, there is a lack of a systematic analysis of interaction between design and sensing performance for conducting specific research tasks in the environment. This lack casts questions on the quality of the data collected during a monitoring task, affecting the scientific effort to better understand our environment [18], [19].

This paper addresses this gap by analyzing the relationship between design, motion stability, sensor data quality, and task effectiveness. Specifically, we focus on performance of in-water sensors directly arising from the extrinsic design and propulsion as the main components.

III. ASV Design

We design an ASV – named *Catabot* with the configuration shown in Fig. 2 – for better in-water monitoring and sensing capabilities, considering the following main criteria:

- **Operable:** The ASV should be operable for 2-4 hours in both fresh and sea waters. It should have robust control modes, such as auto, manual, loiter, etc., and sufficient power supply to sensors, electronics, motors, and controllers under a dynamic environment.
- **Transportable:** The ASV size and weight should allow for easy transportation and deployment. This is crucial especially in work aimed at simultaneously deploying multiple ASVs to monitor and sample algae blooms.
- **Modular:** The ASV is easily assembled and disassembled, since it is constructed from modular parts, either low-cost customized or off-the-shelf. In addition, ASV parts and sensors can be easily moved or modified according to different tasks.

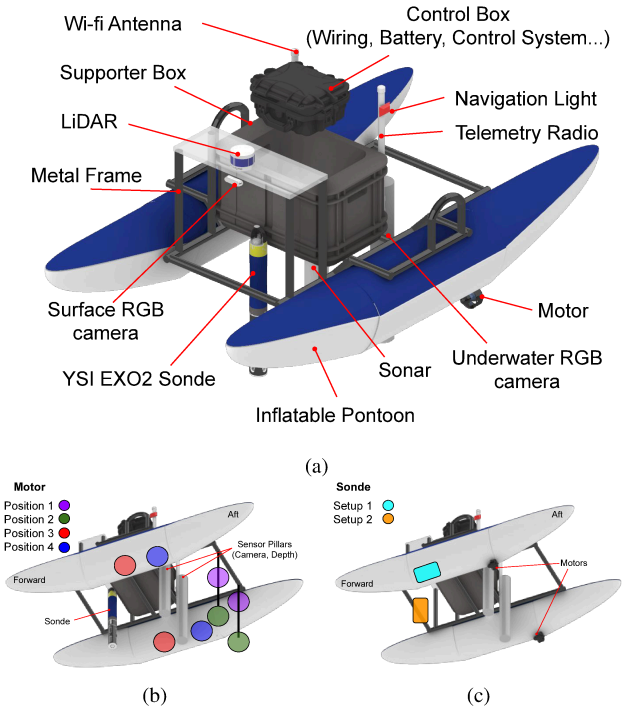

Fig. 2: Overview of *Catabot* **(a)** 3D model (Prospective View) with each component **(b)** Test positions of motors (Bottom View) – ***Position 1***: 7.5 cm motor immersion from the waterline vertically along the end of metal frame, ***Position 2***: 18.0 cm motor immersion from the waterline vertically along the end of metal frame, ***Position 3***: 10.3 cm motor immersion from the waterline under the pontoon transversely parallel to the camera and sonar sensor, ***Position 4***: 9.3 cm motor immersion from the waterline at the edge section between the strait bottom and transom deadrise **(c)** Test setups of sonde (Bottom view) – ***Setup 1***: longitudinal configuration under the pontoon, ***Setup 2***: vertical configuration in front of the supporter box.

- **Stable:** The ASV should be operable under different dynamic environments by having sufficient seaworthiness against motions, such as rolling and pitching. The ASV sensor structures should also be sturdy against disturbances from wind and water dynamics.
- **Reliable:** The ASV design should not hinder the performance of sensor readings. The design and control system should have sufficient integrity to ensure the ASV can engage in autonomous monitoring tasks.

In the following, we describe the main mechanical parts, electronics design, and on-board computer system and communications[1] – important for understanding our design methodology in Section IV.

A. Hull Design

The inflatable catamaran pontoons were chosen as *Catabot*'s physical hull shape. Catamarans are more operable and safer in shallow waters than monohull vehicles, because they have relatively lower draft. The catamaran design enables two

[1]The design and parts for *Catabot* are made opensource on our lab git repository https://github.com/dartmouthrobotics/catabot_design

motors to be symmetrically installed on each side of the structure – detailed in Section III-B.

The overall catamaran weighs about $25\,\mathrm{kg}$, including all other parts such as metal frame. Also, the chosen pontoons can be more compressed and transported, unlike fixed hull types made of carbon or fiberglass. *Catabot* has a versatile storage platform between each pontoon to attach sensors and control box, which includes the electronic components, such as a battery, wiring, distribution, and on-board companion computer. Overall, the operator(s) can assemble and launch *Catabot* within 15 minutes, as tested in our field trials – a benefit from the modular design.

B. Propulsion

We installed a BlueRobotics T200 motor on each side of the hull for a differential drive. The advantage for the selected model is that the motor with simple electrical wiring does not need a sealing structure for the shaft and oil-filled compartment. In addition, a fully-flooded structure with in-water cooling enables the ASV to engage in a long-term task without specific maintenance. A $14.8\,\mathrm{V}$ Li-Po battery powers the two propellers, each providing a forward thrust of $3.69\,\mathrm{kgf}$ given approximately $3000\,\mathrm{RPM}$.

Following the configuration of existing ships with twin screws, we set up *Catabot*'s motors with a symmetrical direction of rotation. Specifically, in case of the forward thrust, the starboard motor has the screw rotating in a clockwise direction, whereas the port motor has the screw rotating in a counter-clockwise direction. This symmetrical design on the catamaran hull not only has better propulsion, but has better course-keeping capability than a monohull design with a single propeller and rudder, which can lead to unbalanced side-wise forces [21]. Each motor has a connection to an Electronic Speed Controller (ESC), which can be controlled by either an RC receiver or an on-board autopilot module. As a result, the motor follows the input signal of Pulse Width Modulator (PWM) ranging from $1100\,\mu\mathrm{s}$ to $1900\,\mu\mathrm{s}$ – where $1500\,\mu\mathrm{s}$ is neutral.

The arrangement of the motors impacts the data collected by the in-water sensors located below the vehicle's keel. This is mainly due to vibration, streamlines, and wave-making resistance on the hull and sensors. We analyze the effects on sensing as per different PWM inputs as well as by motor locations (see Fig. 2 (b)). The analysis described in Section IV will help to improve the data collection performance.

C. On-board Computer System and Communications

For *Catabot* control, we installed a low-level open-source autopilot hardware, Pixhawk. The Pixhawk can use an open-source autopilot software as ArduPilot. Among many ArduPilot branches, we chose to use ArduRover which is compatible with a surface boat using a differential drive. The Pixhawk is connected to a GPS/Compass module, an airspeed sensor, a power module, the two motors, a remote control (RC) receiver, a telemetry radio, and a companion computer.

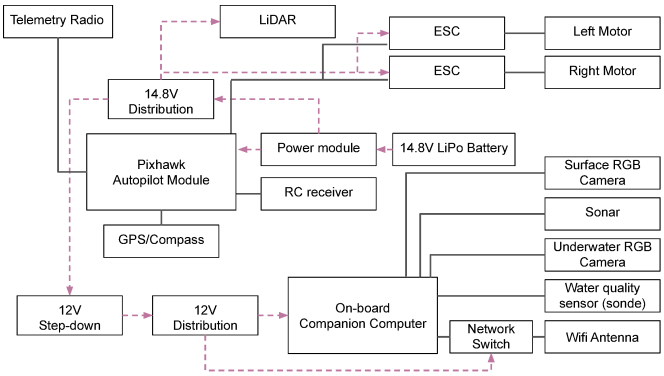

Fig. 3: On-board system schematic block diagram of *Catabot*. Signal wiring (in black solid) and power wiring (in red dotted).

There are three ways that the Pixhawk can control *Catabot* : (1) remote control signal from FrSky Taranis X9D plus to RC receiver X8R via a $2.4\,\mathrm{GHz}$ radio system; (2) ground station control by *Mission Planner* through the telemetry radio operating at $915\,\mathrm{MHz}$; (3) low-level control by Robot Operating System (ROS) node through a USB connection from the companion computer. Telemetry data is recorded on the Pixhawk and sensor data is saved on the companion computer.

This provides a flexible system for roboticists and non-roboticists. If experienced, one can write algorithms and run repeatable experiments via the companion computer. On the other hand, non-specialists can control *Catabot* and set missions through the Mission Planner's graphical user interface.

D. Sensors

Catabot has sensor modules installed either on deck or in water based on purpose or characteristic of data to be collected.

1) On-deck Sensors: GPS/Compass module, Inertial Measurement Unit (IMU), surface RGB Camera, and LiDAR are installed on deck to ensure the best performance by minimizing a blind sector.

The u-blox M8N GPS/Compass module is small and lightweight while also having high performance. This positioning and heading sensor is important to achieve the ASV's autonomous mission and control. The module is connected to the Pixhawk via GPS serial pin and I2C. It is able to receive up to three concurrent signals: GPS, Galileo, Beido, GLONASS). The GPS/Compass module is mounted on top of the control box in Fig. 2 to ensure safe distance from other electromagnetic devices on board.

Second, the IMU built on Pixhawk controller is used to analyze the attitude of *Catabot*. IMU data were analyzed for the field tests described in Section IV. The IMU consists of a main module (MPU 6000 for 3-axis accelerometer/gyroscope), back up modules (L3GD20H for 16 bit gyroscope, LSM303D for 14 bit accelerometer/magnetometer), and a barometer (MEAS MS5611). The processing MCU is a 32bit STM32F427 Cortex-M4F with a 32 bit STM32F103 failsafe co-processor.

Lastly, the Logitech HD webcam and Velodyne LiDAR is used for situational awareness. These two exteroceptive sen-

sors are expected to help *Catabot* perform obstacle avoidance and fully autonomous navigation – a development of our previous work [22]. Given the horizontal field of view (FOV) of the webcam is 78°, we mounted it at the front side of the ASV. Similarly, we installed the Velodyne VLP-16 LiDAR on top of the support frame. It has a 360° horizontal FOV and a 30° vertical FOV with 16 channels.

2) In-water Sensors: underwater RGB camera, sonar, and YSI EXO2 Water Quality Sonde are installed in consideration for optimal data collection. In this study, aside from the intrinsic disturbances occurred by the sensors themselves, we mainly focus on extrinsic factors. These are caused by the relative arrangements of the motors in relation to the locations of the hull and the sensors. The results are investigated in Section IV.

First, the underwater RGB camera (Sony IMX322LQJ-C) captures images in a downward fashion at a max rate of 30 FPS. It has a has a resolution of 5 MP, a horizontal FOV of 80°, and a vertical FOV of 64°. It is connected to the companion computer via USB and is encapsulated inside a sensor pillar with water-proof protection cover. The camera is used to visually monitor and analyze water quality with a focus on color, particles, and biological entities.

Second, the sonar (echo sounder) sensor observes the water depth. The sonar (CruzPro ATU120AT) based on NMEA0183 serial data can measure the depth up to 140 m from the sensor. The sonar is connected to companion computer via USB. We mounted the underwater camera (left) and the sonar sensor (right) on each side of ASV from the center line of the vehicle.

Lastly, the YSI EXO2 sonde monitors water quality at a 1 Hz rate. In particular: chlorophyll, pH, optical dissolved oxygen, water temperature, conductivity, turbidity, salinity, and pressure. We made a sonde interface module to communicate between the sonde and the companion computer via USB. A ROS node[2] can interface with the sonde through the companion computer to monitor and record real-time sonde data. In addition as back-up, the sonde has an internal memory to store data.

E. Design Space

Based on the prototype design with all the aforementioned components (Fig. 2 (a)), our design space was focused on the location of motors (Fig. 2 (b)) and sensors (Fig. 2 (c)). These are the main underwater components for a surface vehicle [23].

First, motor positions are designed by symmetrical configuration with respect to the center line of *Catabot*. To ensure effective propulsion, we avoided a motor position closer to the bow over the longitudinal center of the body frame. The design space for motors are then circumscribed to four locations, depending on an original on-board structure or an additional support structure, e.g., metal bar, made by an operator where the motors can be installed – see Fig. 2 (b). Positions 1 and 2 required the metal frame, whereas for Positions 3 and 4, motors were attached on the direct bottom sections of the pontoons.

[2]The code is made opensource on our lab git repository https://github.com/dartmouthrobotics/ysi_exo

Fig. 4: *Catabot* at the pool for hydrostatic test.

Parameter	Value
Length, Beam (Overall) [m]	2.4, 1.4
Draft Forward, Aft [m]	0.056, 0.064
Displacement [kgf]	25
Trim [deg]	0.5
Wetted Surface Area [m^2]	0.865
Weight to Immerse [kfg/cm]	12.245

TABLE I: Particulars of *Catabot*.

Next, in-water sensor positions are designed. We symmetrically – with respect to the center line – attached the underwater RGB camera and sonar to the rigid supporter box. This makes ASV collect relevant images of the bottom in connection with the water depth value. Based on this configuration of two sensors, we designed sonde positions. Setup 1 is a longitudinal configuration attached on the bottom side of *Catabot* while Setup 2 is a vertical configuration at the front of the ASV body. The experimental analyses based on these sonde Setups help scientists to compare the sensing performance in practice.

IV. Analysis Methodology and Results

We conducted hydrostatic tests in a pool (Fig. 4) and in simulation. Our proposed methodology consists of monitoring how changes in design – locations of motors and sensors – affect motion stability and sensor interference based on particulars of the proposed modular research-oriented ASV in Table I. At the end, we report the results of the simulation and field testing experiments.

A. Hydrostatics

With the full *Catabot* setup described in the previous section, we conducted hydrostatic tests in simulation, with a *Catabot* model made in the CAD software *Rhino 6*, and in the pool. The goal is to observe the static stability and fundamental tests for equilibrium. First, the initial measurements (displacement, draft, trim, heel, draft change by additional weights, ...) in the pool test were checked for consistency of the model property done in the simulation. Under normal weight conditions, the *Catabot* in the pool had a forward and aft draft as 0.0560 m and 0.0640 m, respectively, while in simulation the weight analysis showed forward and aft draft as 0.0548 m and 0.0630 m, respectively. When loading a 10 kg object, the result of the pool test showed forward and aft draft as 0.0650 m and 0.0710 m, respectively, while the simulation showed forward and aft draft as 0.0629 m and 0.0716 m, respectively.

With this method, in case of future design shifts (e.g., new sensor installation or movement), the resultant model equilibrium can be predicted by cross-checking actual data from ASV or vice versa. Since the heel and trim angle changes

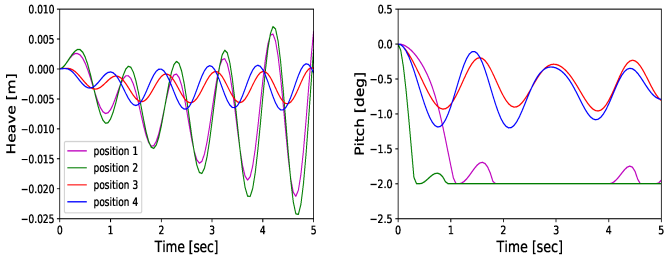

Fig. 5: Forward motion CFD simulation as per different locations of propellers. (upper) Heave. (lower) Pitch.

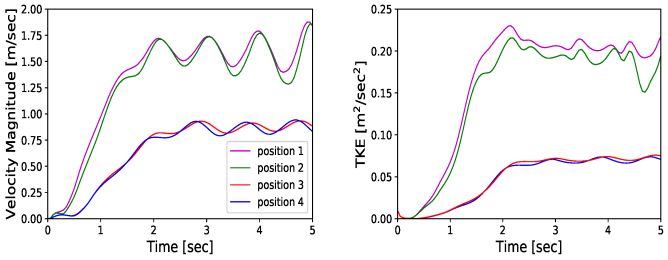

Fig. 6: Sensor interference CFD simulation as per different locations of propellers. (upper) Velocity magnitude. (lower) TKE.

are contingent on the model's design and weight distribution, one should avoid excessive loads by the design shifts.

B. Stability

Unlike typical safety analysis on ship's translation and rotation motions [24]–[26], we measure stability in terms of pitch and heave with different arrangements of sensors and motors. The goal is to minimize the motion's amplitude and equilibrium time, which would overall minimize negative effects on the sensor readings. Given the above calculated hydrostatic data (dimension of ASV, draft, trim, displacement, ...), the righting arm/breadth ratio is large enough to range between 0.28 and 0.36 while *Catabot* rolls up to 45 degrees. The righting arm is defined as the distance between the center of gravity and the center of buoyancy. The breadth is defined as maximum distance over the extreme points on the left and right side of the ASV body. The relationship between the two parameters is a determinant factor for intact stability, e.g., a 192-meter car-carrier with 0.028 for the righting arm/breadth ratio [27]. Thus, note that rolling is negligible given the catamaran hull design choice.

We fixed the location of the in-water sensors (camera, echo sounder, and sonde) and tested different motor positions, as shown in Fig. 2 (b). The left motor is set at $-1500\,\mathrm{RPM}$ and the right motor is at $3000\,\mathrm{RPM}$. The values of RPM were chosen based on the maximum throttle ($3000\,\mathrm{RPM}$) and half of the maximum reverse throttle ($-1500\,\mathrm{RPM}$), in order to make *Catabot* gradually turn in a circular track. This unbalanced setting is to help show how the *Catabot* motions are related to the sensor noises under non-trivial maneuverings. Trivial maneuverings, such as going forward or backward, are neglected for quantitative analysis of the attitudes, since the robot only has translation motions along the x-axis with no rotational motions. After $5\,\mathrm{s}$ of maneuvering, the results in Fig. 5 showed that Positions 3 and 4 have a lower amplitude of the heave and pitch than Positions 1 and 2. This implies that Positions 3 and 4 can have relatively more stable quality of environmental measurement data in case the other conditions are the same.

C. CFD Simulation

We tested sensor interference caused by discharged waters from direct interactions with motor locations. Under the same stability test conditions, we monitored Turbulent Kinetic Energy (TKE) and velocity magnitude near the left sensor (underwater camera) due to the wake of the propellers. Since TKE is proportional to fluctuations of turbulence, a large TKE can deteriorate the sensor data quality, introducing disturbances in readings [28]. By using TKE as the main parameter, we can quantitatively predict the sensor interference caused by the motor arrangements.

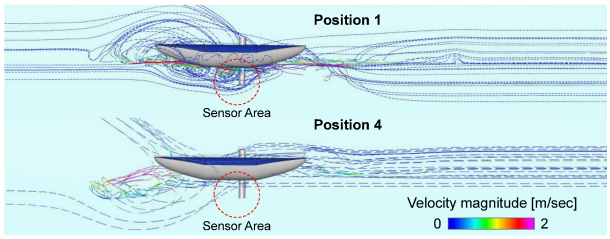

Fig. 7: Streamline analysis as per different locations of propellers (upper) Position 1 case. (lower) Position 4 case.

In Fig. 6, TKE of Positions 1 and 2 is over three times greater than that of Positions 3 and 4. This means that for the same measuring spot of the sensor pillar in Fig. 2, Position 3 and 4 will have more stable data than Position 1 and 2, because of the water turbulence and velocity.

We performed an additional experiment: the ASV rotates in place by setting the left and the right motor to $-3000\,\mathrm{RPM}$ and $3000\,\mathrm{RPM}$, respectively, for $2\,\mathrm{s}$. The values of RPM were chosen based on the maximum throttle for forward ($3000\,\mathrm{RPM}$) and backward ($-3000\,\mathrm{RPM}$). This motion is modelled according to a case when *Catabot* make a sharp turn at a waypoint during a water monitoring task. Qualitatively, we observed the streamlines generated around the hull. Given similar characteristics in motion and TKE analysis between Positions 1 and 2 and between Positions 3 and 4, we mainly compared the cases for Positions 1 and 4. In Fig. 7, Position 1 has higher concentration and magnitude of streamlines than Position 4, impairing sensor performance.

D. Field Test 1 - Motor Position

The main goal of the field tests is to analyze in practice the sensor interference affected by motor positions and controls, all while under dynamic environments. This will validate the simulation experiments carried out with the CFD.

1) Testing Environment: In sea waters – see Fig. 8 (a) – which is a dynamic environment, we tested a prototype *Catabot* design under the same configurations as Section IV-C and finalized a motor position. The testing location was

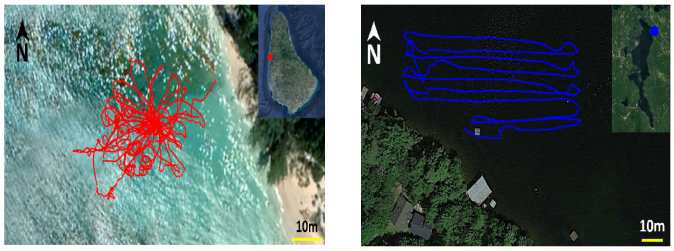

(a) (b)

Fig. 8: Testing environment. **(a)** sea waters at west coast of Barbados (red dot) and ASV's track (red lines) **(b)** lake waters at Herrick cove of Lake Sunapee (blue dot) and ASV's track.

within about $500\,\mathrm{m}$ from the GPS coordinate $13°\,11'\,28''\,N$, $148°\,59'\,39''\,W$ (home position) in the west coast of Barbados. We considered the region to be a relatively favorable environment because of the semi-diurnal tide cycles, the small changes in tidal heights, and the small magnitude tidal currents. The tidal height was around $+/-\ 0.5\,\mathrm{m}$ from Mean Low Lower Water level during the period from Jan 13 to Jan 15 2020. To test *Catabot* under consistent external conditions, we chose experimental time approximately one hour before or after the daily slack waters. The low-tide water height was about $0.2\,\mathrm{m}$, while the high-tide water was about $0.8\,\mathrm{m}$. The weather conditions during testing dates were an average temperature of $25°$ to $30°$ and a wind speed of $8\,\mathrm{m/s}$ to $12\,\mathrm{m/s}$ from the easterly direction.

For this test, we used a customized script based on MAVROS commands and communicated with the *Catabot* through Wi-Fi and telemetry. Specifically, from the home position, we sent an overriding PWM signal[3] to each motor, i.e., the left motor through servo Ch.1 and the right motor through servo Ch.3, as shown in Fig. 9. Note that PWM channel is reversely mapped at the left motor for symmetrical rotation as described in Section III-B. This testing is categorized into four different control phases: moving forward by symmetric PWM signals to both motors (*control 1*), moving backward by negative to both motors (*control 2*), turning to the left by high PWM to the right motor and low PWM to the left motor (*control 3*), and turning to the right by high PWM to the left motor and low PWM to the right motor (*control 4*). In addition, we tested *Catabot* with motor Positions 1, 3, and 4 – Position 2 is excluded being similar to Position 1 and displaying poor performance in simulation.

2) Qualitative Results: For comparing sensor interference, a diver took videos of the underwater hull side. We extracted image frames from the videos and determined level of interference visually from the bubbles and blurriness. Fig. 10 shows that during *control 3*, Position 1 had the worst visible discharge current. Compared to the other two motor positions, Position 1 had relatively less motor immersion ratio from the water surface, causing cavitation. Cavitation itself can lead to bad effects on propulsion efficiency and can cause

[3]PWM and RPM conversion data are available at https://bluerobotics.com/store/thrusters/t100-t200-thrusters/t200-thruster/

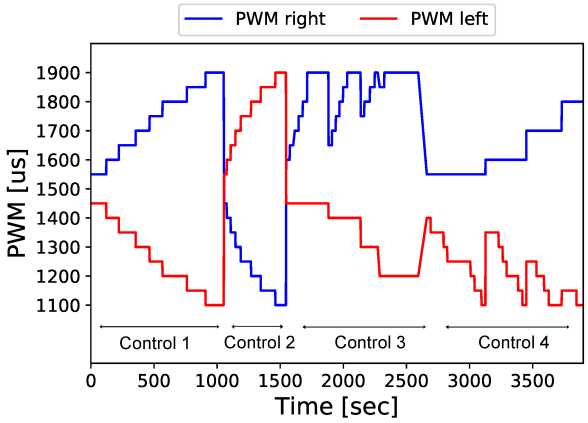

Fig. 9: Example of PWM signal inputs during about one-hour test. ***Control 1***: moving forward by symmetric PWM signals to the left (L) and the right (R) motor, e.g., 1100 PWM on L as about $3000\,\mathrm{RPM}$ and 1900 PWM on R as about $3000\,\mathrm{RPM}$. ***Control 2***: moving backward by negatively symmetric PWM signals to L and R motor, e.g., 1900 PWM on L as about $-3000\,\mathrm{RPM}$ and 1100 PWM on R as about $-3000\,\mathrm{RPM}$. ***Control 3***: turning to the left by unbalanced PWM signal to L (low) and R (high) motor, e.g., 1300 PWM on L as about $1800\,\mathrm{RPM}$ and 1800 PWM on R as about $2500\,\mathrm{RPM}$. ***Control 4***: turning to the right by unbalaned PWM signals to the L (high) and R (low) motor, e.g., 1200 PWM on L as $2500\,\mathrm{RPM}$ and 1700 PWM on R as $1800\,\mathrm{RPM}$.

machinery damage [29], which should be avoided regardless of the interference with in-water sensors.

Moreover, we compared images from the underwater camera during *control 2*. As shown in Fig. 11 (a), in case of Position 1, the camera rarely captures the sandy seabed due to more prominent interference (e.g., bubbles). The images presented many bubbles or discharge currents. However, as shown in Fig. 11 (b), in case of position 4, the camera was able to capture the sandy seabed more clearly .

3) Quantitative Results: Analyses are based on saved data from the rosbag files on the on-board companion computer and from the telemetry log files on the ground control station. The following results in Fig. 9 are based on one hour comparisons as per PWM signal.

First, the rotational ego-motion is analyzed along the y-axis of the robot body frame, i.e., pitch as conducted in CFD tests. Fig. 12 shows that the robot tends to have a *trim by the head* in the real environment. This is based on the interaction between the pontoon (hull) and the water [30]. *Catabot* does not have on-board ballasting systems, which is common on commercial vessels. For this reason, based on the design factor only, *Catabot* has the least pitch angle as well as the reasonably less deviation of it by using the motor Position 4 than the other positions. Position 3 also has a small deviation of the pitch angles, but the robot has the largest *trim by the head* (see Root Mean Square (RMS) in Fig. 12 (b)). Therefore, it is best to avoid this option to gain better maneuverability and efficiency from pontoon-motor interaction.

Next, the depth measurements of the sonar sensor are analyzed. Here, the depth measurement is defined as the distance

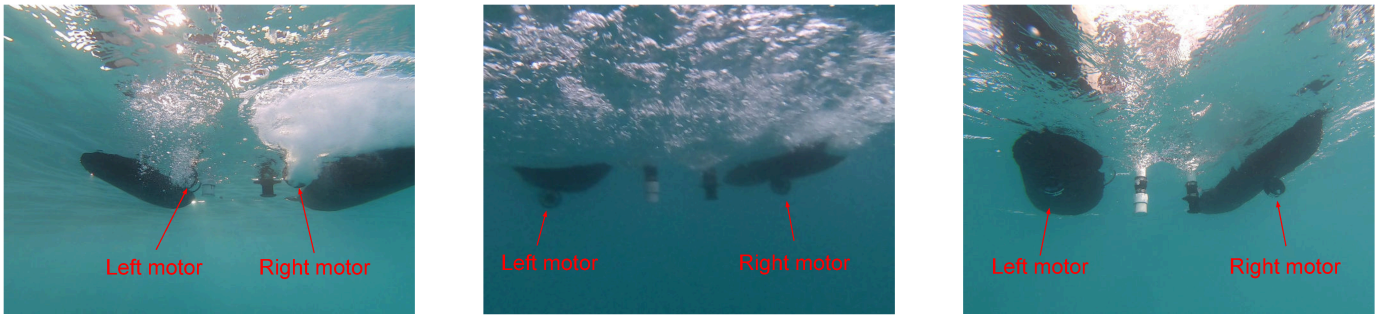

(a) (b) (c)

Fig. 10: Qualitative comparison of image frames taken by a diver during the left turning maneuver (*control 3)*. The images were taken from the stern side of the robot. **(a)** Position 1 **(b)** Position 3 **(c)** Position 4.

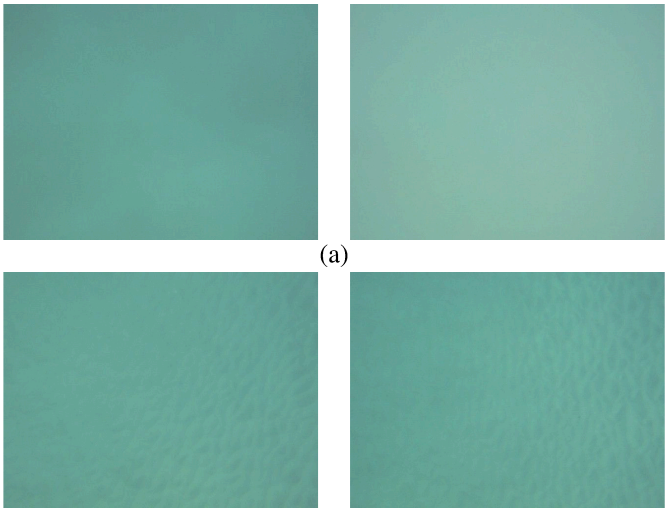

(a)

(b)

Fig. 11: Qualitative comparison of image frames taken by robot's own underwater camera during backward maneuver (*control 2)*. The images capture the sandy seabed. **(a)** Position 1 – interference by bubbles and discharge currents **(b)** Position 4 – clearer view.

from the transducer to the seabed, i.e., Under Keel Clearance (UKC). As shown in Fig. 13, one can observe that the choice of motor positions also affect the depth sensor performance. (1) Position 4 has the smallest ratio of invalid data with respect to total number of sensor data points, under the same time and ASV control conditions. When the sensor was not able to receive a reflected signal from the seabed, it returned a -1 as an invalid datum. (2) Among the valid data only, Position 4 also has the least overshooting data ratio. As shown in Fig. 13 (a)-(c), when the sensor received an unstable signal, e.g., multiple-time reflection from the seabed, the invalid or overshooting data ratio increased. Overall, Position 4 returned the smallest Standard Deviation (SD) and RMS during the field tests.

E. Field Test 2 - Sonde Setup

1) Testing Environment: In lake waters – see Fig. 8 (b) – as a controlled/stable environment, we validated the proposed design and modular changes, i.e., new sensor installations, for the purpose of lake monitoring. In particular, to monitor algae blooms in the lake, we installed a YSI EXO2 sonde as described in Section III-D on board the prototype *Catabot*. The testing location was within about $300\,\mathrm{m}$ from the GPS coordinate $43°\,24'\,35''\,N,\ 72°\,02'\,12''\,W$ in Herrick Cove of Lake Sunapee, NH. The weather conditions during testing dates were with temperatures between $15\,°\mathrm{C}$ to $20\,°\mathrm{C}$ and wind speeds between $1\,\mathrm{m/s}$ to $3\,\mathrm{m/s}$ from a westerly direction.

2) Testing Results: We tested configurations of the sonde sensor as shown in Fig. 2 (c) – Setup 1 is a longitudinal installation under the pontoon, Setup 2 is a vertical installation in front of the support box. *Catabot* followed a West-East directional lawnmower path (see Fig. 8 (b)) with velocity of $1\,\mathrm{m/s}$ while in auto mode. We mainly tested the interference on the *chlorophyll* sensor equipped on the sonde, because of its sensitivity and significance to algae bloom monitoring. Fig. 14 (a) shows that the *chlorophyll* measurements depends on the position of sonde installation. Setup 1 has more data variation, i.e., unexpected data jumps than the sonde Setup 2.

V. Discussion

Two main factors that affect sensor data quality are water dynamics caused by motor locations and general ASV motion. We chose Position 4 as the final configuration of the motors, due to its low variation of motions and low image blurriness on the camera sensor. It also best optimizes the motion stability and minimizes the interference on the sensors. Unlike Position 3, Position 4 is shown to be more effective in maneuvering and in propulsion as trim is closer to even keel.

Based on the final design, we chose to install the new water quality sensor using Setup 2 for aquatic monitoring tasks. This vertical arrangement of the sensor along the center-line of the ASV was shown to have the smallest interference on the probe sensors, e.g., chlorophyll.

While the analysis was on a catamaran hull boat, this analysis provides more general insights that can be applied in other contexts. As validated in field trials, it is clear that different designs can affect the quality of the collected data. Quantitative metrics captured such adverse effects on sensors. We expect that the proposed methodology and metrics can be adopted to evaluate a new design criterion, i.e., sensor reliability. Practical considerations to determine the design

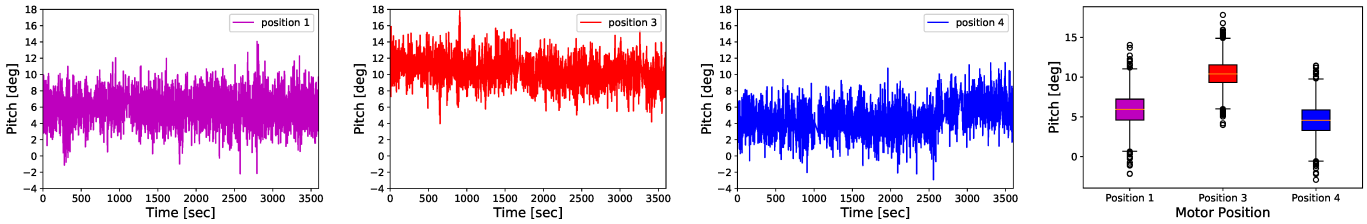

(a) (b) (c) (d)

Fig. 12: Analysis of pitch as per different locations of motors during the field test. The pitch measurement topic from imu data was subscribed at approximately 4.0 Hz rate. **(a)** Position 1 – RMS: 6.2328, SD: 2.0179, max: 14.0504 **(b)** Position 3 – RMS: 10.5747, SD: 1.7218, max: 17.8204 **(c)** Position 4 – RMS: 5.0256, SD: 1.9749, max: 11.4492 **(d)** box plot comparison.

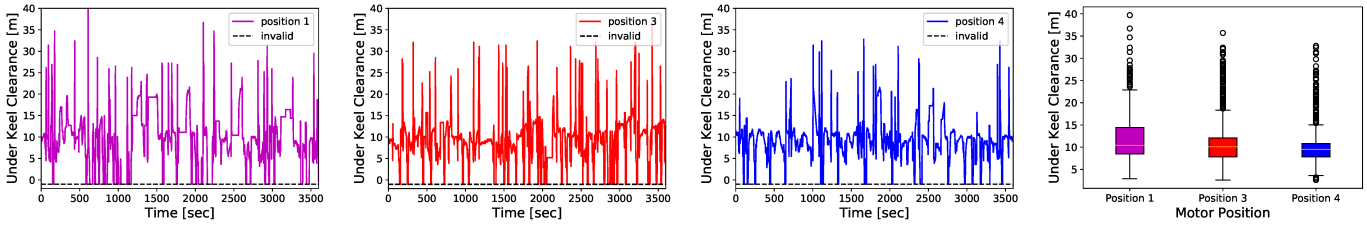

(a) (b) (c) (d)

Fig. 13: Analysis of UKC by sonar as per different locations of motors during the field test. -1 is invalid value of sonar from false signal. The sonar measurement topic was subscribed at approximately 0.7 Hz rate. *: ratio with respect to total number of data points, **: ratio with respect to number of valid data. **(a)** Position 1 – number of total data points: 2582, number of valid data: 2163 (83.77%*), number of invalid data: 419 (16.23%*), number of overshooting data: 118 (5.45%**), SD: 4.9398, RMS: 12.5576 **(b)** Position 3 – number of total data points: 2599, number of valid data: 2310 (88.88%*), number of invalid data: 289 (11.12%*), number of overshooting data: 94 (4.07%**), SD: 4.4079, RMS: 11.3012 **(c)** Position 4 – number of total data points: 2528, number of valid data: 2358 (93.28%*), number of invalid data: 170 (6.72%*), number of overshooting data: 74 (3.14%**), SD: 3.6280, RMS: 10.5122 **(d)** box plot comparison.

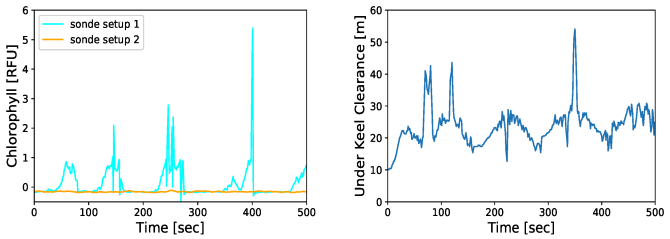

(a) (b)

Fig. 14: In-water sensor measurements in lake waters. **(a)** Analysis of Chlorophyll measurement as per different location of sensors during the field test. The sonde measurement topic was subscribed at approximately 1 Hz rate. Setup 1 was tested on April 25, 2020 – RMS: 0.5690, SD: 0.5577. Setup 2 was tested on May 17, 2020 – RMS: 0.1596, SD: 0.0144 **(b)** Analysis of UKC by sonar during the field test operation on May 17, 2020 – RMS: 24.3544, SD: 5.8835.

space can be extracted as well from the paper – draft, heel, trim, propulsion moment, intact stability, fixed body structure constrain the motor locations.

Computational design techniques can be used to automate and find the optimized boat design. Currently, we are optimizing second *Catabot* design aimed for water quality monitoring performed together with the first *Catabot*. In the near future, a fleet of multi ASVs will be optimized by the computational algorithm which is applied with the scheme in this paper – the modular design, particular design space for motor and sensors, and systematic validation metrics.

Despite the optimized design, the the collected data might still experience some issues in its quality, as shown in Fig. 14 (b). The reason can be that the robot needs to avoid a certain control behavior or the robot needs to choose an adaptive path to minimize the inference in operation. Further studies on optimized designs are required to explore how motion factors (e.g., throttle, speed, turning rate) and different planned paths impact data fluctuation and measurement quality.

VI. Conclusion and Future Work

In this paper, we proposed a novel approach to optimize the design of a research-oriented ASV, to modularize the configuration, and to enable simple deployment and recovery. Following 3D modelling with hydrostatic and CFD tests, we validated the design through field experiments (in sea waters and in lake waters) to measure differences in sensor data according to various designs. While many operate ASVs, our study is the first to analyze the effects of the design on in-water sensors. The proposed method was applied to *Catabot* with a water quality sensor to monitor cyanobacterial blooms. Moreover, our qualitative and quantitative analysis methodology is applicable to other ASV design configurations made for any autonomous in-water data collection tasks e.g., coral reef surveying. Our proposed methodology will enable optimization of motion stability and sensor performance, while reducing unnecessary time and effort to accomplish missions.

We are pursuing three main directions to optimize the future iterations of this methodology. First, we plan to develop an algorithm for optimizing controls during a monitoring task with the proposed design. We are also designing an adaptive path for monitoring cyanobacterial blooms, which the ASV will strictly follow while complying to the aforementioned criteria for a consistent monitoring task. As a long-term goal, we will develop a computational algorithm that, given certain specifications, will automatically optimize the ASV design for deploying simultaneously multiple ASVs.

ACKNOWLEDGMENT

The authors would like to thank the National Science Foundation for its support (NSF 1923004, NSF 1919647).

REFERENCES

[1] International Maritime Organization, *SOLAS: International Convention for the Safety of Life at Sea, 74: 97/98 amendments*. 1999.

[2] Germanischer Lloyd, "Guidelines for Sea Trials of Motor Vessels," *Rules for Classification and Construction*, 2012.

[3] CLL: International Maritime Organization, 66/88, *International Convention on Load Lines*. 2003.

[4] E. I. Sarda, H. Qu, I. R. Bertaska, and K. D. von Ellenrieder, "Station-keeping control of an unmanned surface vehicle exposed to current and wind disturbances," *Ocean Engineering*, vol. 127, pp. 305–324, 2016.

[5] J. Moulton, N. Karapetyan, S. Bukhsbaum, C. McKinney, S. Malebary, G. Sophocleous, A. Quattrini Li, and I. Rekleitis, "An Autonomous Surface Vehicle for Long Term Operations," *MTS/IEEE OCEANS Charleston*, pp. 1–10, 2018.

[6] P. H. Heins, B. L. Jones, and D. J. Taunton, "Design and validation of an unmanned surface vehicle simulation model," *Applied Mathematical Modelling*, vol. 48, pp. 749–774, 2017.

[7] J. Jung, J. Park, J. Choi, and H. Choi, "Autonomous mapping of underwater magnetic fields using a surface vehicle," *IEEE Access*, vol. 6, pp. 62 552–62 563, 2018.

[8] H. Ferreira, C. Almeida, A. Martins, J. Almeida, N. Dias, A. Dias, and E. Silva, "Autonomous bathymetry for risk assessment with ROAZ robotic surface vehicle," *MTS/IEEE OCEANS Bremen*, pp. 1–6, 2009.

[9] P. H. Heins, B. L. Jones, and D. J. Taunton, "Design and validation of an unmanned surface vehicle simulation model," *Applied Mathematical Modelling*, vol. 48, pp. 749–774, Aug. 2017.

[10] M. A. Schoener, "Global estimation methodology for wave adaptation modular vessel dynamics using a genetic algorithm," Master's thesis, Embry-Riddle Aeronautical University, Apr. 2019.

[11] M. Bibuli, G. Bruzzone, M. Caccia, and L. Lapierre, "Path-following algorithms and experiments for an unmanned surface vehicle," *Journal of Field Robotics*, vol. 26, no. 8, pp. 669–688, 2009.

[12] E. Desa, P. K. Maurya, A. Pereira, A. M. Pascoal, R. G. Prabhudesai, A. Mascarenhas, E. Desa, R. Madhan, S. G. P. Matondkar, G. Navelkar, S. Prabhudesai, and S. Afzulpurkar, "A small autonomous surface vehicle for ocean color remote sensing," *IEEE Journal of Oceanic Engineering*, vol. 32, no. 2, pp. 353–364, 2007.

[13] J. H. Bae, S. Luo, S. S. Kannan, Y. Singh, B. Lee, R. M. Voyles, M. Postigo-malaga, E. G. Zenteno, L. P. Aguilar, and B.-c. Min, "Development of an Unmanned Surface Vehicle for Remote Sediment Sampling with a Van Veen Grab Sampler," *MTS/IEEE OCEANS Seattle*, pp. 1–7, 2019.

[14] M. Dunbabin and A. Grinham, "Experimental evaluation of an autonomous surface vehicle for water quality and greenhouse gas emission monitoring," in *IEEE International Conference on Robotics and Automation*, 2010, pp. 5268–5274.

[15] J. Wang, W. Gu, and J. Zhu, "Design of an autonomous surface vehicle used for marine environment monitoring," *International Conference on Advanced Computer Control, ICACC 2009*, pp. 405–409, 2009.

[16] P. Kimball, J. Bailey, S. Das, R. Geyer, T. Harrison, C. Kunz, K. Manganini, K. Mankoff, K. Samuelson, T. Sayre-McCord, F. Straneo, P. Traykovski, and H. Singh, "The WHOI Jetyak: An autonomous surface vehicle for oceanographic research in shallow or dangerous waters," *IEEE/OES Autonomous Underwater Vehicles, AUV*, pp. 1–7, 2015.

[17] N. C. Lin, M. Benjamin, C. F. Chen, H. C. Wang, Y. C. Hsiao, Y. W. Huang, C. T. Hung, T. K. Chuang, P. W. Chen, J. T. Huang, C. C. Hsu, and A. Censi, "Duckiepond: An Open Education and Research Environment for a Fleet of Autonomous Maritime Vehicles," in *IEEE/RSJ International Conference on Intelligent Robots and Systems (IROS)*, Nov. 2019, pp. 7219–7226.

[18] G. Hitz, F. Pomerleau, M. È. Garneau, C. Pradalier, T. Posch, J. Pernthaler, and R. Y. Siegwart, "Autonomous inland water monitoring: Design and application of a surface vessel," *IEEE Robotics and Automation Magazine*, vol. 19, no. 1, pp. 62–72, Mar. 2012.

[19] L. Pedersen, T. Smith, S. Y. Lee, and N. Cabrol, "Planetary LakeLander-A Robotic Sentinel to Monitor Remote Lakes," *Journal of Field Robotics*, vol. 32, no. 6, pp. 860–879, Sep. 2015.

[20] J. E. Manley, "Unmanned surface vehicles, 15 years of development," *MTS/IEEE OCEANS Quebec*, pp. 1–4, 2008.

[21] J. Longo and F. Stern, "Effects of drift angle on model ship flow," *Experiments in Fluids*, vol. 32, pp. 558–569, 2002.

[22] M. Jeong and A. Quattlini Li, "Risk Vector-based Near miss Obstacle Avoidance for Autonomous Surface Vehicles," in *IEEE/RSJ International Conference on Intelligent Robots and Systems (IROS)*, 2020, (In press).

[23] A. Papanikolaou, "Holistic ship design optimization," *CAD Computer Aided Design*, vol. 42, no. 11, pp. 1028–1044, Nov. 2010.

[24] I. Senjanović, J. Parunov, and G. Ciprić, "Safety analysis of ship rolling in rough sea," *Chaos, Solitons & Fractals*, vol. 8, no. 4, pp. 659–680, 1997.

[25] S. Surendran and J. Venkata Ramana Reddy, "Numerical simulation of ship stability for dynamic environment," *Ocean Engineering*, vol. 30, no. 10, pp. 1305–1317, Jul. 2003.

[26] A. Maki, Y. Akimoto, Y. Nagata, S. Kobayashi, E. Kobayashi, S. Shiotani, T. Ohsawa, and N. Umeda, "A new weather-routing system that accounts for ship stability based on a real-coded genetic algorithm," *Journal of Marine Science and Technology*, vol. 16, no. 3, pp. 311–322, Sep. 2011.

[27] S. Surendran and J. Venkata Ramana Reddy, "Numerical simulation of ship stability for dynamic environment," *Ocean Engineering*, vol. 30, no. 10, pp. 1305–1317, Jul. 2003.

[28] M. Visonneau, E. Guilmineau, P. Queutey, J. Wackers, and G. B. Deng, "Assessment of statistic and hybrid LES turbulence closures for complex free-surface flow simulation with combined grid refinement criteria," *30th Symposium on Naval Hydrodynamics*, pp. 2–7, 2014.

[29] A. Peters, U. Lantermann, and O. el Moctar, "Numerical prediction of cavitation erosion on a ship propeller in model- and full-scale," *Wear*, vol. 408-409, pp. 1–12, Aug. 2018.

[30] A. Härting, A. Laupichler, and J. Reinking, "Considerations on the squat of unevenly trimmed ships," *Ocean Engineering*, vol. 36, no. 2, pp. 193–201, Feb. 2009.